Journal of Applied Polymer Science

Application of response surface methodology to evaluate the effect of dry-spinning parameters on poly (ε-caprolactone) fiber properties

Bahareh Azimi,[1,2] Parviz Nourpanah,[1] Mohammad Rabiee,[3] Shahram Arbab,[4] Maria Grazia Cascone,[2] Andrea Baldassare,[2] Luigi Lazzeri[2]

[1]Department of Textile Engineering, Amirkabir University of Technology, 424 Hafez Ave, Tehran, 15875-4413, Iran
[2]Department of Civil and Industrial Engineering, University of Pisa, largo Lucio Lazzarino 1 56122, Pisa, Italy
[3]Department of Biomedical Engineering, Amirkabir University of Technology, Tehran, Iran
[4]Department of Textile Engineering, ATMT Research Institute, Amirkabir University of Technology, Tehran, Iran
Correspondence to: B. Azimi (E-mail: azimi89@aut.ac.ir)

ABSTRACT: Poly (ε-caprolactone) fibers were prepared by dry-spinning method. The effect of processing parameters on linear density, mechanical, and morphological properties of fibers was investigated using the response surface methodology (RSM). This method allowed evaluating a quantitative relationship between polymer concentrations, spinning speed, and draw ratio on the properties of the fibers. Polynomial regression model was fitted to the experimental data to generate predicted response. The results were subjected to analysis of variance to determine significant parameters. It was found that all three parameters had significant effect on linear density of fibers. Combined effect of concentration and spinning speed was observed in which the linear density of fiber was more sensitive to changes in the solution concentration at lower spinning speed. Polymer concentration had the largest influence on the mechanical properties of fibers. An average cross-sectional radius of fibers was affected by concentration and draw ratio in opposite manner. Among all three parameters, only polymer concentration had significant effect on circularity of fiber cross sections. By applying the RSM, it was possible to obtain a mathematical model that can be used to better define processing parameters to fabricate dry-spun PCL fiber in a more rational manner. © 2015 Wiley Periodicals, Inc. J. Appl. Polym. Sci. **2015**, *132*, 42113.

KEYWORDS: biomedical applications; extrusion; fibers

Received 15 August 2014; accepted 12 February 2015
DOI: 10.1002/app.42113

INTRODUCTION

Poly (ε-caprolactone) (PCL) is a synthetic biodegradable aliphatic polyester which has attracted considerable research attention in recent years, notably in the specialist biomedical areas.[1] It can be spun to fibers for subsequent fabrication of desirable textile structures. Due to excellent characteristics, such as biodegradability, biocompatibility, mild undesirable host reactions, and three-dimensional structures, PCL fibers, whose diameter ranges from nanometer to millimeter, are broadly studied in biomedical area. In fiber form, PCL and its copolymers have been investigated as drug delivery systems,[2] 'long-lasting' absorbable sutures,[3] and 3-D scaffolds for tissue engineering applications.[4] Extrusion of PCL into monofilaments and multifilaments may be achieved by fiber formation mechanisms, such as melt spinning,[5] electrospinning,[6] and solution spinning.[7] There are distinct features of each of these processes that are subsequently reflected in fiber properties. The solution spinning methods, dry-spinning, and wet-spinning, are usually utilized for polymers that do not melt. In both methods polymer is dissolved into a suitable solvent and the polymer solution pumped through the spinneret. In dry-spinning, fiber is obtained through solvent evaporation, while in wet-spinning, fiber is obtained through a phase inversion mechanism in which the polymer solution gets in contact with a fluid that is miscible with the spinning solvent but is not a solvent for the polymer.[8] Some studies have used solution spinning to produce PCL fibers for different biomedical applications. Williamson *et al.* produced PCL fibers using a wet-spinning technique.[7] Cell attachment and proliferation were investigated on these fibers for tissue engineering application. PCL fibers were produced by wet-spinning from solutions in acetone under low shear (gravity flow) conditions. Fibers were found to exhibit low tensile modulus and high extensibility.[9] A hydrophilic macromolecule and a lipophilic drug were incorporated into PCL fibers by gravity spinning using particulate dispersions and co-solutions of PCL and steroid, respectively. The low shear and temperature condition were advantageous for avoiding shear or heat-induced degradation of pharmaceuticals.[2] The antibiotic gentamicin sulphate was incorporated in gravity-spun PCL fibers by

spinning from particulate suspensions of the drug in PCL solution to produce a controlled delivery system.[10] An additive manufacturing technique for the fabrication of three-dimensional polymeric scaffolds, based on wet-spinning of PCL or PCL/hydroxyapatite solutions was developed by Puppi *et al.*[11]

Many factors and variables can affect the ultimate properties of fibers obtained via solution spinning. These variables can be separated in three categories namely polymer solution parameters, processing conditions and ambient parameters like temperature and humidity. In recent years, effect of wet-spinning parameters on different properties of fibers has been studied through experimental observations.[12–14] For example, Puppi *et al.*[15] have optimized wet-spinning techniques to produce PCL fibrous scaffolds loaded with bisphosphonate and hydroxyapatite. The wet-spinning process for obtaining the PCL-based wet-spun fibers was investigated by improving the processing conditions, such as the solvent–nonsolvent system, polymer concentration, and solution feed rate. On the basis of this preliminary investigation, the optimized processing conditions were 15% w/v polymer concentration, acetone as solvent, ethanol as nonsolvent and 1.75 mL/h flow rate.[15] However, application of dry-spinning method and the knowledge on the influence of its parameters on the properties of PCL fibers through theoretical simulations is lacking. In dry-spinning process, some factors such as polymer concentration, solvent evaporation, relaxation, and spinning-line stress in the air gap between spinneret and collecting bobbin can influence fiber properties. Two dominant factors, elongational, and shear stresses have a dramatic effect on the polymer segmental orientation and relaxation at the outer surface of the fiber.[16,17]

In this study, a simple dry-spinning method was used to produce PCL fiber. The mild production conditions (air gap room temperature without using nonsolvent) can be benefits of this method to produce PCL fibers for subsequent drug delivery application. The effects of solution concentration, spinning speed and draw ratio on linear density, mechanical and morphological properties of fibers were systematically investigated using RSM. This method is a powerful statistical technique for testing multiple variables because fewer experimental trials are needed as compared to the "one-factor-at-a-time" method. Moreover, the use of this model allows a straightforward and systematic representation of the processing parameters influencing fiber formation, and can be used to predict the results of the experiments applying different combinations.[18]

MATERIALS AND METHODS

Material

PCL with average molecular weight of 80 kDa and dichloromethane (DCM) as solvent were purchased from Sigma-Aldrich (Milan, Italy) and used as received.

Fiber Production

Weighed amounts of PCL equal to 20, 25, and 30 g were added, respectively, to 80, 75, and 70 g of DCM to obtain 20, 25, and 30 wt % solutions. The PCL was dissolved in DCM at room temperature for about 24 h under mechanical stirring until homogeneous solutions formed.

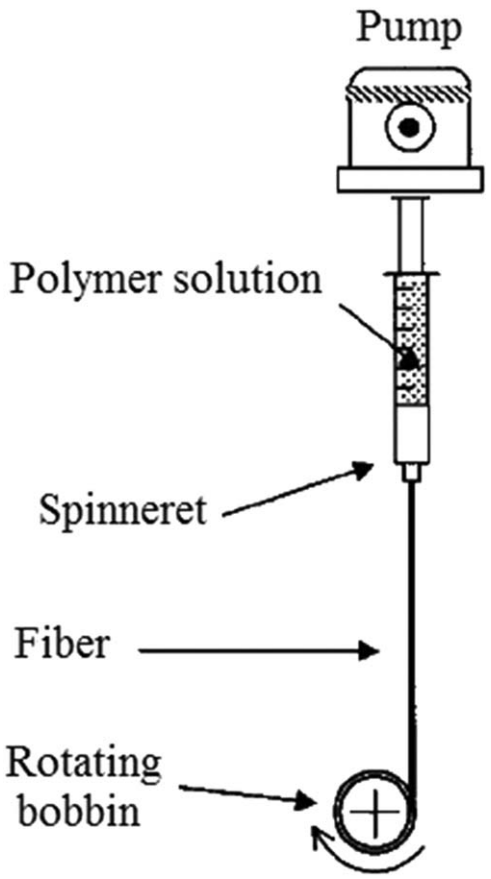

Figure 1. Scheme of the spinning apparatus used to produce PCL microfibres.

The polymer solution was stored at room temperature without disturbance for 12 h to remove the shear effect of stirring and fine air bubbles entrapped in the solution. Microfibers were produced by a dry-spinning process in which the polymer solution was forced through a needle with a diameter of 0.65 mm. As the polymer solution exits from the spinneret, a fiber is formed due to solvent evaporation in the air gap (10 cm) between the spinneret and the collecting bobbin. Draw ratio, defined as the ratio of take-up to extrusion velocity. By varying the rotational speed of the bobbin, fibers with different draw ratios were obtained. The spinning apparatus, schematically represented in Figure 1, allowed obtaining fiber length in the range 10–15 m.

Experimental Design

The formation of fibers from solution differs from the formation from the melt by one more important point. In fiber formation from melt, the main parameters of fiber solidification are filament temperature and diameter profiles, with the other process variables playing a somewhat auxiliary role. If the velocity of take-up and rate of extrusion are constant, then the rheological properties govern the attenuation of the filament diameter. The diameter profile is a result of the temperature profile and its influence on the rheological properties of the

Table I. Coded and Actual Levels of the Design Factors

		Real values of the coded levels		
Variable	Code	−1	0	1
Concentration (wt %)	A	20	25	30
Spinning speed (cm/s)	B	3	5	7
Draw ratio	C	5	6	7

polymer. Constant cooling conditions, with the other parameters constant, determine the actual temperature profile.[19] In fiber formation from solution, solvent diffusion is further factor which has important effect on fiber formation mechanism. The removal of solvent, in a dry process, or wet is governed by the rate of diffusion and the filament diameter. The diffusivity depends on the temperature and polymer concentration.[19] Therefore, in dry-spinning process, parameters that influence solvent diffusion and evaporation significantly affect final properties of fiber. In this study, the effect of polymer concentration (wt %), spinning speed (cm/s), and draw ratio, on PCL fiber properties was investigated by applying a full-factorial face centered central composite design (CCD) using RSM (Design Expert 8.0.7.0, Stat-Ease). The CCD is one of designs in RSM that can be very useful in the optimization process, since it estimates the major effects and interactions that can be used to predict an optimum combination of factors by suggested model.

A CCD has three groups of design points including factorial, axial, and center points. All point descriptions will be in terms of coded values of the factors. For statistical calculations, the variables were coded to lie ±1 for factorial and axial points and 0 for the center points. The experimental range and coded levels of independent variables are presented in Table I.

In preliminary experiments we determined the experimental boundaries for fiber formation by changing the concentration, spinning speed, and draw ratio. In dry-spinning method, when the solvent removal from the fiber is rapid in relation to the velocity of the solvent diffusion from the fiber core towards its surface, a sheath of solid or almost solid polymer may be formed around a relatively low concentrated solution core. When this takes place, further solvent removal is additionally complicated by the necessity of solvent osmosis through a layer of solid, or almost solid, polymer. Such a course of events is also behind the mechanism which causes the fibers to have noncircular cross section.[19] Therefore, high solution concentration ranges were considered, in order to have lower amount of solvent inside the solution and subsequently have fibers with circular cross sections. Lower concentrations (<20 wt %), lead to formation of fiber with very flat and undesirable cross section shape. The same rationale was used to select the spinning speed and draw ratio ranges. Within the given boundaries (Table I), in all cases fibers can be produced. A three-factor CCD design with a total of 20 runs, including 8 factorial points, 6 axial points, and 6 replicates at the center points, was used to fit a second-order response surface in order to investigate the effect of process factors on different properties of fibers. The experimental conditions are shown in Table II.

The responses could be related to the selected variables by a second-order polynomial regression model as given by the following equation:

$$Y = b_0 + \sum_{i=1}^{k} b_i x_i + \sum_{i=1}^{k} b_{ii} x_i^2 + \sum_{i=1}^{k-1} \sum_{j=i+1}^{k} b_{ij} x_i x_j + e_i \qquad (1)$$

where Y represents the predicted response, k is the number of the factors, x_i and x_j are the coded values of independent variables, b_0, b_i, b_{ii}, b_{ij} are the intercept, linear, squared, and interaction coefficients of the model, respectively. e_i is the random error or residual associated to the experiments, which is assumed to follow a normal distribution with zero mean and variance equal (1) across all values of Y.[20] This equation can be used to locate the optimum for the set of independent variables by putting the partial derivatives of the model response with respect to the individual model coefficients equal to zero.[21] Statistical significance of the model and the regression coefficients were estimated by ANOVA combined with the application of Fisher's F test as well as Student's t test. The probability values (P value) are utilized to consider the statistical significance of the determined model, with a threshold value of $P < 0.05$. The accuracy of the model was also checked by the coefficient of determination R-squared (R^2) as the measure of goodness of fit

Table II. Experimental Design Layout of Central Composite Design with the Independent Variables, A: Concentration (wt %), B: Spinning Speed (cm/s), and C: Draws Ratio

	Independent variables			Coded values		
Sample label	A	B	C	A	B	C
F_1	25	5	6	0	0	0
F_2	25	3	6	0	−1	0
F_3	25	5	6	0	0	0
F_4	25	5	6	0	0	0
F_5	25	5	6	0	0	0
F_6	20	7	7	−1	1	1
F_7	20	5	6	−1	0	0
F_8	30	3	5	1	−1	−1
F_9	20	3	7	−1	−1	1
F_{10}	30	7	5	1	1	−1
F_{11}	30	3	7	1	−1	1
F_{12}	20	7	5	−1	1	−1
F_{13}	25	5	6	0	0	0
F_{14}	30	7	7	1	1	1
F_{15}	25	5	5	0	0	−1
F_{16}	25	5	7	0	0	1
F_{17}	20	3	5	−1	−1	−1
F_{18}	25	7	6	0	1	0
F_{19}	30	5	6	1	0	0
F_{20}	25	5	6	0	0	0

Table III. Analysis of Variance for Linear Density of Fibers

Source	Sum of squares	*df*	Mean square	*F* value	*P* value Prob > *F*	
Model	431.56	9	47.95	69.92	<0.0001	Significant
$R^2 = 0.9844$						
$R^2_{adj} = 0.9703$						
$R^2_{pred} = 0.8978$						
Adequate precision = 35.887						
A Concentration (wt %)	220.62	1	220.62	321.71	<0.0001	Significant
B Spinning speed (cm/s)	31.01	1	31.01	45.22	<0.0001	Significant
C Draw ratio	163.94	1	163.94	239.07	<0.0001	Significant
AB	5.88	1	5.88	8.58	0.0151	
AC	2.69	1	2.69	3.92	0.0757	
BC	0.051	1	0.051	0.075	0.7902	
A^2	1.39	1	1.39	2.02	0.1853	
B^2	7.12	1	7.12	10.39	0.0091	
C^2	1.51	1	1.51	2.20	0.1689	
Residual	6.86	10	0.69			
Lack of fit	4.32	5	0.86	1.70	0.2863	Not significant
Pure error	2.54	5	0.51			
Cor total	438.42	19				

of the model. When R^2 approaches unity, the empirical model fits the actual data. The regular R^2 can be artificially inflated by simply continuing to add terms to the model, even if the terms are not statistically significant. Thus, a large value of R^2 does not necessarily imply that the regression model is consistent. To take this into account, an adjusted R^2 (R^2_{adj}) is defined by eq. (2), which is generally considered to be a more accurate measure than R^2:

$$R^2_{adj} = 1 - \frac{n-1}{n-m-1}\left(1-R^2\right) \quad (2)$$

where n is the number of observations and m is the total number of regression coefficients.[21] The R^2_{adj} plateaus when insignificant terms are added to the model. Predicted R^2 (R^2_{pred}) is a measure of the amount of variation in new data explained by the model and it will decrease when there are too many insignificant terms. A rule of thumb is that R^2_{adj} and R^2_{pred} values should be within 0.2 of each other. The relationships between the response and the variables were also visualized by three-dimensional response surfaces to see the relative influence of the parameters and predicted experimental results for other combinations as well.[22]

Characterization

Linear Density. Fiber linear density (λ_m) (expressed in tex) was determined in accordance with ASTM D 1577-01.

Mechanical Properties. Fibers with gauge length of 10 mm were clamped and drawn with a rate of 25 mm/min on tensile machine (Instron 5542) up to rupture and their mechanical characteristics were determined. For each sample at least six replicates were characterized and the average values reported. Fiber was clamped by means of grips (Instron 2712-Series Pneumatic Action Grips) specially designed for delicate samples of small size, such as films or filaments. The pneumatic action of the grips allows a maximum load capacity of 5 N, and allows compensating variations in sample thickness during the test. The load cell used for the tensile tests has a maximum capacity of 5 N.

Morphological Properties. To calculate the surface area to volume ratio (SVR) and circularity (C) of the fibers, the image analysis of scanning electron microscopy (SEM) images was conducted in Photoshop CS-5 software (5 measurements per image were taken). Fibers were freeze fractured in liquid nitrogen, sputter coated with a thin gold layer, and observed by a scanning electron microscope (JEOL JSM-5600 LV) with voltage of 10 kV.

RESULTS AND DISCUSSION

Linear Density of Fibers

The thickness or diameter of a fiber is one of its most fundamental properties. However, the cross section of some fibers is not circular, so sometimes it is not possible to measure the diameter of a fiber in any meaningful way. Because of this problem, a system of denoting the fineness of a fiber by weighing a known length of it has evolved. This quantity is known as the linear density and it can be measured with a high degree of accuracy if a sufficient length of fiber is used.[23] There is a nice distinction between the meaning of fineness and diameter. Fineness does not imply a specific geometrical shape for the fiber cross section while diameter generally dose.[24] The direct system of denoting linear density is based on measuring the weight per unit length of a fiber. The main units in use are tex, decitex, and denier. In this work, the cross section of fibers was not

Table IV. Analysis of Variance for the Refined Model of Linear Density

Source	Sum of squares	*df*	Mean square	*F* value	*P* value Prob > *F*	
Model	421.46	4	105.36	93.17	<0.0001	Significant
$R^2 = 0.9613$						
$R^2_{adj} = 0.9510$						
$R^2_{pred} = 0.9280$						
Adequate precision = 39.522						
A Concentration (wt %)	220.62	1	220.62	195.09	<0.0001	
B Spinning speed (cm/s)	31.01	1	31.01	27.42	0.0001	
C Draw ratio	163.94	1	163.94	144.97	<0.0001	
AB	5.88	1	5.88	5.20	0.0376	
Residual	16.96	15	1.13			
Lack of fit	14.43	10	1.44	2.84	0.13	Not significant
Pure error	2.54	5	0.51			
Cor total	438.42	19				

completely circular and varied depending on the processing conditions. Therefore, linear density was used as fineness of fibers. To evaluate the influences of solution concentration, spinning speed, and draw ratio on linear density of fibers, the design matrix of experimental conditions with the corresponding response values was fitted to a polynomial model. Based on the results of the sequential model, sum of squares and the calculated statistics for all model terms, a quadratic model was suggested. The mathematical equation proposed for this response (in terms of actual values) is:

$$\lambda_m = -32.08 + 3.48A - 3B + 7.53\,C - 0.08\,AB - 0.11\,AC + 0.04\,BC - 0.028A^2 + 0.4B^2 - 0.7C^2 \quad (3)$$

The ANOVA results of the regression model are shown in Table III. *F* value of 69.92 implies that the model is significant. The significance of the model was also determined using the "Lack

Table V. Different Properties of Fibers Obtained from Experiments and Predicted from the Models

	Linear density (tex)		Tensile strength (Mpa)		Young's modulus (Mpa)		r_{av}		Circularity	
Sample lable	Exp	Pred	Exp	Pred	Exp	Pred	Exp	Pred	Exp	Pred
F_1	23.98	24.06	57.61	64.03	189.95	193.24	70.98	76.18	0.76	0.77
F_2	28.65	25.82	41.22	41.73	106.027	140.7	74.47	76.18	0.79	0.77
F_3	22.46	24.06	66.63	64.03	219.38	193.24	70.67	76.18	0.79	0.77
F_4	24.04	24.06	69.73	64.03	202.77	193.24	66.8	76.18	0.69	0.77
F_5	23.93	24.06	79.57	64.03	193.16	193.24	66.6	76.18	0.82	0.77
F_6	15.00	14.41	62.74	60.47	179.25	168.25	47.63	48.43	0.59	0.57
F_7	19.00	19.36	35.15	50.13	131.73	164.99	53.91	55.63	0.60	0.57
F_8	36.13	35.42	37.09	44.95	160.46	168.95	88.84	95.43	0.76	0.80
F_9	16.83	16.22	37.09	38.51	142.49	112.45	45.04	48.43	0.54	0.57
F_{10}	30.55	30.19	73.28	66.91	202.71	224.75	87.00	95.43	0.82	0.80
F_{11}	26.16	27.33	68.58	66.31	164.47	168.95	76.58	81.03	0.84	0.80
F_{12}	22.33	22.51	35.6	39.11	147.07	168.25	56.32	62.83	0.56	0.57
F_{13}	23.44	24.06	57.61	64.03	170.71	193.24	73.47	76.18	0.81	0.77
F_{14}	22.18	22.09	84.95	88.27	247.03	224.75	70.18	81.03	0.78	0.80
F_{15}	27.85	28.11	57.7	53.35	187.2	193.24	83.75	83.38	0.84	0.77
F_{16}	19.40	20.01	81.75	74.71	208.61	193.24	61.76	68.98	0.75	0.77
F_{17}	23.20	24.31	24.61	17.15	130.1	112.45	57.29	62.83	0.62	0.57
F_{18}	23.30	22.30	60.91	63.69	205.87	196.5	64.85	76.18	0.78	0.77
F_{19}	28.31	28.76	70.3	77.93	238.55	221.49	77.96	88.23	0.83	0.80
F_{20}	24.53	24.06	63.43	64.03	189.95	193.24	72.18	76.18	0.76	0.77

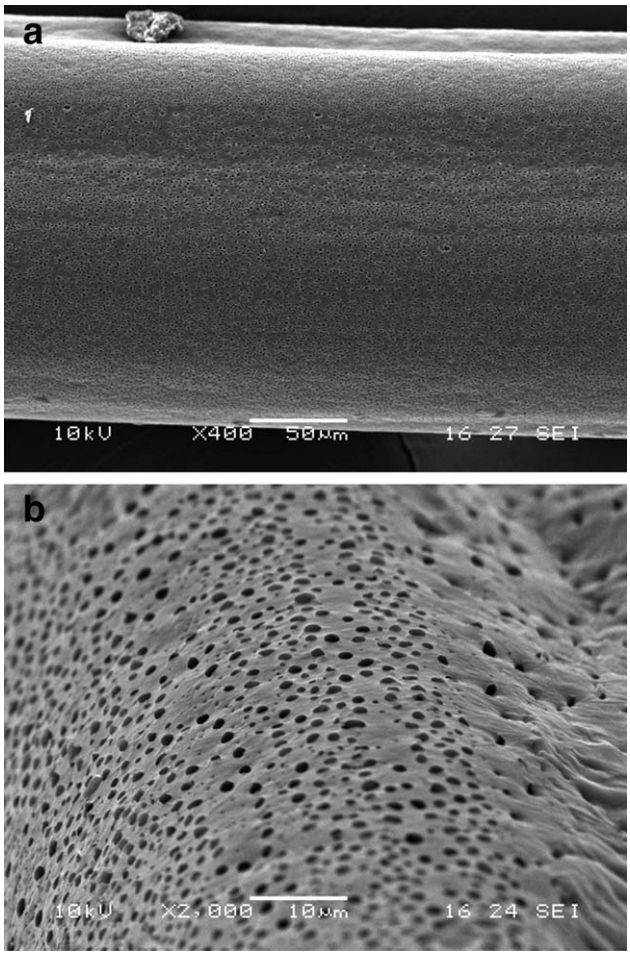

Figure 2. SEM micrographs of the fiber surface prepared from a 20 wt % solution, spinning speed of 3 cm/s and draw ratio of 5. (a) 400×, (b) 2000×.

of fit" test which compares the residual error (from the model error) to the pure error (from replicated experiments) and measures how well the model fits the data. Significant lack of fit ($P < 0.05$) indicates that the model does not fit the data well.[25] In this case, the model shows statistically insignificant lack of fit, as is evident from the P value of 0.2863. The lack of fit F value of 1.70 shows the validity of the predictive model which can be used to calculate linear density from eq. (3). "Adequate precision" measures the signal to noise ratio. The ratio of 35.887 indicates an adequate signal (a ratio greater than 4 is desirable). The R^2 of 0.9844 shows the model is highly reliable. The R^2_{pred} of 0.8978 is in reasonable agreement with the R^2_{adj} of 0.9703.

The significance of each polynomial term was checked using F test and its associated probability, P value. Values of "Prob > F" less than 0.05 indicate that the term is significant. In this case, concentration (A), spinning speed (B), draw ratio (C), and combination of concentration, and spinning speed (AB) were significant model terms. Eliminating the remaining not significant terms (AC, BC, A^2, B^2, and C^2) from the starting general polynomial expression allowed the model to be refined and a new set of terms to be obtained as follows:

$$\lambda_m = +18.55 + 1.36A + 1.26B - 4.04\,C - 0.085\,AB \qquad (4)$$

Analyzing the ANOVA results after model reduction for this response shows that R^2 of 0.9613 with an R^2_{adj} (0.9510), is in more reasonable agreement with the R^2_{pred} (0.9280). The model F value (93.17) and adequate precision (39.522) have been improved due to the model adjustment (Table IV). The linear density of fibers obtained from experiments at different processing conditions and predicted linear density from the model are presented in Table V. The values determined were in agreement with the predicted values, which suggest that the model was accurate. The significance of regression coefficients can determined on the basis of their P value. The smaller the P value, the bigger the significance of the corresponding coefficient.

It can be seen by the results given in Table IV that all three parameters are still significant. The importance of the variables and their effects can be also explained by their F value. The F value of factor A (195.09) is bigger than the F value of factor B (27.42), and C (144.97). Therefore, solution concentration (A) is the major factor affecting the linear density followed by draw ratio and spinning speed, in the order. Solvent evaporation is one of the strong directional fields to kinetically freeze nanostructures under proper preparation conditions. The solvent evaporation process can

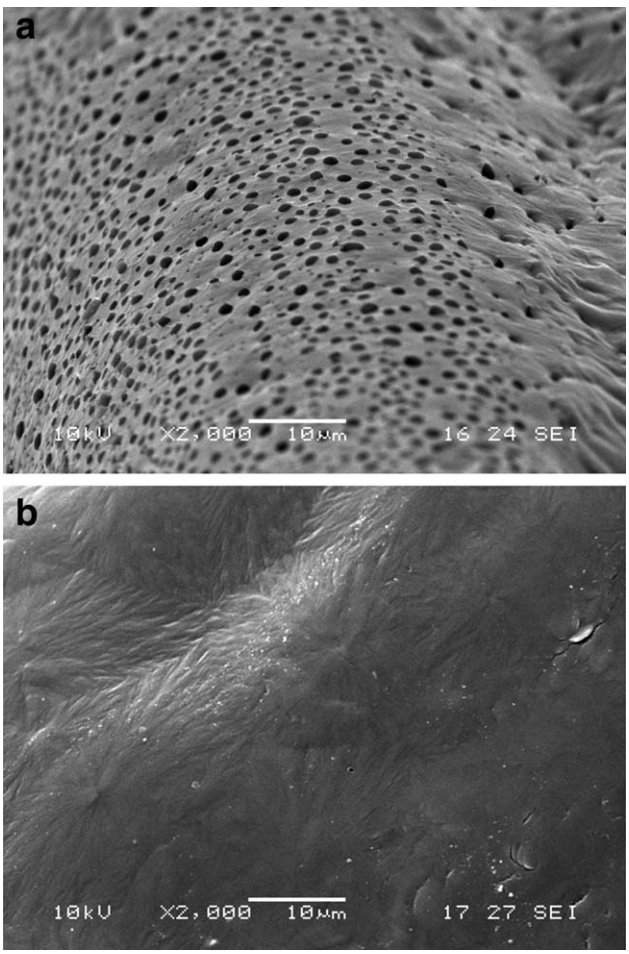

Figure 3. Effect of solution concentration on surface porosity of fibers produced at spinning speed of 3 cm/s, draw ratio of 5 and solution concentration of (a) 20 wt %, (b) 30 wt %.

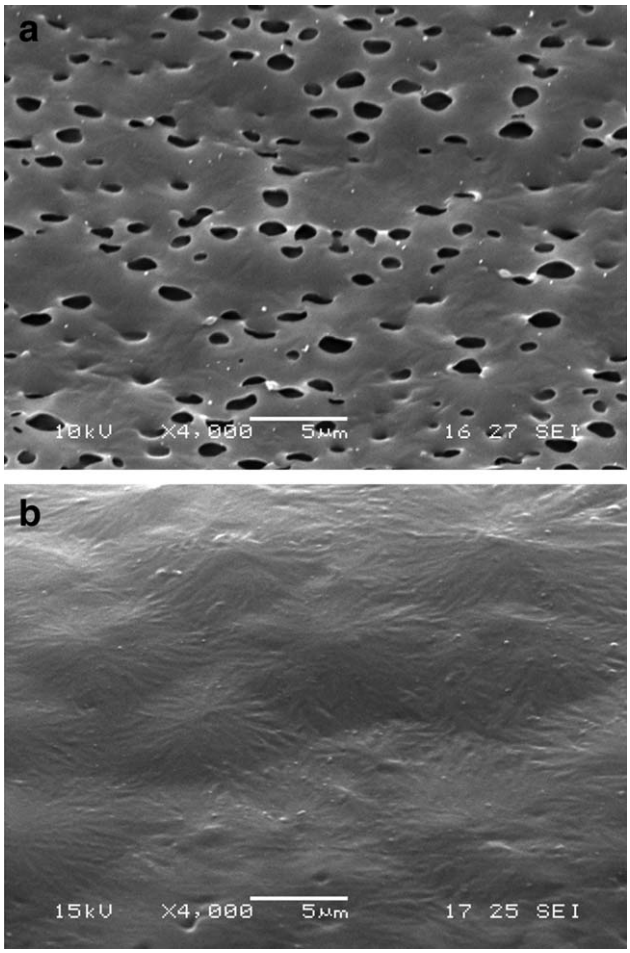

Figure 4. SEM micrographs of fiber surface prepared from 25 wt % solution, draw ratio of 6 and different spinning speed (a) 3 cm/s, (b) 7 cm/s.

produce ordered arrays of cylindrical microdomains oriented normal to the surface of fibers (Figure 2).

This happens because of the gradient in the solvent concentration from the air interface into the inner part of the fiber during drying.[26] Mutually destructive effect of the extensional stress caused by drawing and the shear stress may disturb the formation and shape of the pores. Increasing solution concentration has lead to a decrease in surface porosity of fibers (Figure 3). A variation in the bulk solution concentration changes the relaxation behavior and solvent concentration gradient between outer surface and inner parts of the fibers. Consequently, the rate of solvent evaporation is different in the same air gap distance for different solutions spun under the same spinning speed.[14] Increasing polymer concentration reduce diffusion coefficient of solvent and air. In low diffusion coefficient values, the polymer chains have enough mobility and time to heal surface pores. Therefore, higher solution concentrations result in lower surface porosity and higher linear density of fibers. Moreover, at higher solution concentration, there is a higher population of polymer chains per unit volume of the fiber, which result in a higher linear density.

The variation of spinning speed can have two opposite effects on linear density of fibers as follows.

First, the effect of spinning speed on surface porosity. In dry-spinning, the variation of the spinning speed changes the amount of DCM which can evaporate before arriving to the take up roller. It is noteworthy that surface porosity, pore size distribution and shape of the nanoscopic porous are influenced by evaporation time of the solvent.[14] As it can be seen in Figure 4, at higher spinning speed, no pores were observed on the surface of fiber. Decreasing of spinning speed, which is coupled to increasing the solvent evaporation time, leads to formation of a nanoporous arrays on the surface and to a decrease in the linear density of the fibers.

Second, the effects of spinning speed on polymer chain entanglement. Increasing the spinning speed leads to a higher shear stress as well as higher shear rate at the spinneret. Polymer solutions normally show shear thinning behavior, i.e., their viscosity decreases by increasing shear rate and time of shear.[27] Since the viscosity of any polymeric solution is primarily due to its highly entangled molecular chain network, any change in entanglement density of this network leads to change in the viscosity. The entanglement density changes as the polymer is put under relaxed or stressed conditions. Under higher shear rate, the chains tend to come out of the entanglements and the viscosity decreases. This shear thinning behavior of the polymer solution is helpful during the spinning process as the fluidity of the solution increases due to the shear experienced by it during extrusion processes. The decreasing fiber linear density at higher

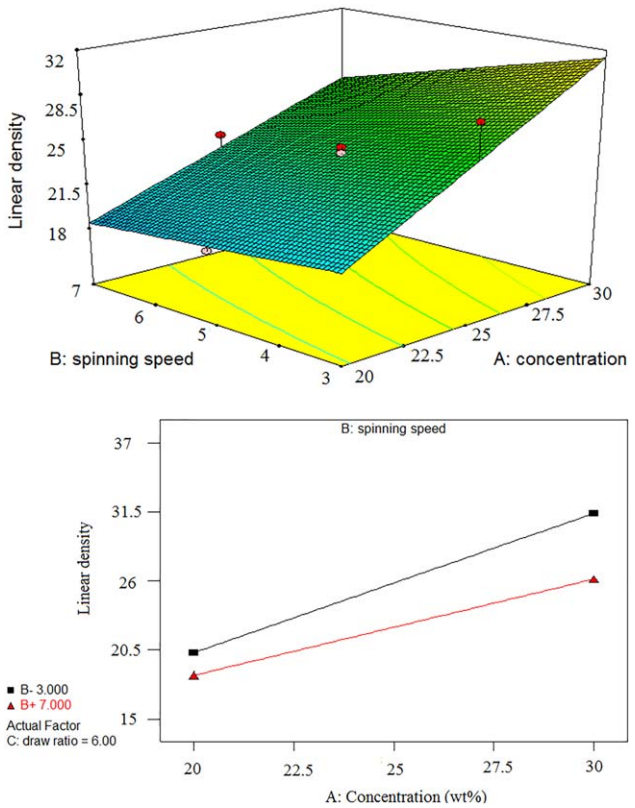

Figure 5. Response surface (a) and interaction plots (b) of the combined effects of solution concentration and spinning speed on linear density. [Color figure can be viewed in the online issue, which is available at wileyonlinelibrary.com.]

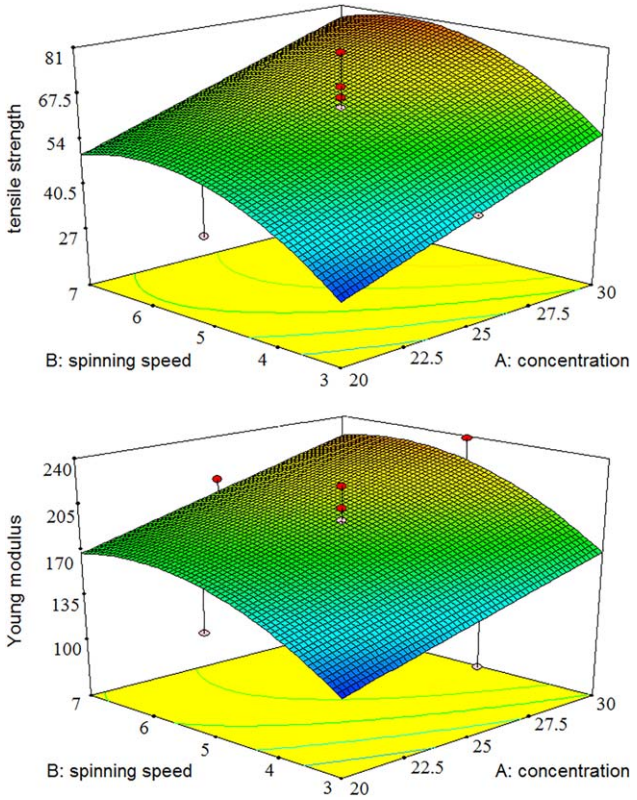

Figure 6. Response surface of the combined effects of solution concentration and spinning speed on (a) tensile strength and (b) Young's modulus. [Color figure can be viewed in the online issue, which is available at wileyonlinelibrary.com.]

spinning speed can be due to the easier stretching of jets in the applied draw ratio at lower viscosities. Figure 5 revealed that the spinning speed had more considerable effect on polymer chain entanglement than on surface porosity. Therefore, the linear density of fiber has finally decreased by increasing of spinning speed. However, the mild curve slope represents two adverse effects of spinning speed on linear density of fibers.

An interaction occurs when the response varies belong the settings of two factors. This indicates that the effect of one factor depends on the level of the other one.[21] From the statistical analysis (Table IV), the interdependence of solution concentration and spinning speed on linear density was significant. Response surface and interaction plots of solution concentration and spinning speed are shown in Figure 5(a,b), respectively. As it can be seen in these figures, the linear density of fiber was more sensitive to changes in the solution concentration at lower spinning speed. At higher spinning speeds, there were no surface porosity in any applied polymer concentrations, so variation of linear density by concentration was just dependent on the variation of polymer chains population. The higher the concentration, the higher population of polymer chains in the volume unit of the fiber and the higher linear density. As shown in Figure 3, at lower spinning speeds, surface porosity has decreased due to increasing of polymer concentration. So, at lower spinning speed, variation of linear density by concentration was simultaneously dependent on variation of polymer chains population and surface porosity of fibers. Therefore, the linear density of fiber was more sensitive to changes in lower spinning speed. These results show that the combination of solution concentration and spinning speed can be used to control the linear density of fiber. Increasing draw ratio, lead to reduction of thickness as well as linear density of fiber as expected.

Mechanical Properties

The designed experiments using CCD were performed and a quadratic model was fitted to the results of tensile strength and Young's modulus as responses. Adequate quadratic models for prediction of the response variables are given by the following equations:

$$\text{Tensile strength} = -74.28 + 19.32A + 29.14B - 85.47C + 0.19AB + 0.08AC - 0.32BC - 0.36A^2 - 2.67B^2 + 7.96C^2 \quad (5)$$

Table VI. Analysis of Variance for the Adjusted Model of Tensile Strength (Mpa)

Source	Sum of squares	*df*	Mean square	*F* value	*P* value Prob > *F*	
Model	4902.44	4	1225.61	20.07	<0.0001	Significant
$R^2 = 0.8426$						
$R^2_{adj} = 0.8006$						
$R^2_{pred} = 0.7340$						
Adequate precision = 18.156						
A Concentration (wt %)	1932.38	1	1932.38	31.64	<0.0001	
B Spinning speed (cm/s)	1185.70	1	1185.70	19.42	0.0005	
C Draw ratio	1141.26	1	1141.26	18.69	0.0006	
B^2	643.09	1	643.09	10.53	0.0054	
Residual	916.04	15	61.07			
Lack of fit	570.53	10	57.05	0.83	0.6288	Not significant
Pure error	345.51	5	69.10			
Cor total	5818.48	19				

Table VII. Analysis of Variance for the Adjusted Model of Young's Modulus (Mpa)

Source	Sum of squares	*df*	Mean square	*F* value	*P* value Prob > *F*	
Model	18773.78	3	6257.93	14.06	<0.0001	Significant
$R^2 = 0.7250$						
$R^2_{adj} = 0.6734$						
$R^2_{pred} = 0.5275$						
Adequate precision = 11.891						
A Concentration (wt %)	7985.15	1	7985.15	17.94	0.0006	
B Spinning speed (cm/s)	7749.71	1	7749.71	17.41	0.0007	
B^2	3038.93	1	3038.93	6.83	0.0188	
Residual	7121.13	16	445.07			
Lack of fit	5824.75	11	529.52	2.04	0.2244	Not significant
Pure error	1296.38	5	259.28			
Cor total	25894.91	19				

$$\text{Young's modulus} = 329.71 + 3.4A + 46.54B - 144.27C + 0.87AB + 0.069AC + 3.69BC - 0.05A^2 - 7.66B^2 + 11.30C^2 \quad (6)$$

The ANOVA results show that the *P* values of *A*, *B*, *C*, and B^2 for tensile strength and the *P* values of *A*, *B*, and B^2 for Young's modulus are smaller than 0.05. So, these variables have significant effect on the tensile strength and Young's modulus of fibers, respectively. In order to improve the model, the insignificant coefficients (*AB*, *AC*, *BC*, A^2, *and* C^2 for tensile strength) and (*C*, *AB*, *AC*, *BC*, A^2, and C^2 for Young's modulus) were eliminated and the final models were refined as follows:

$$\text{Tensile strength} = -167.75 + 2.78A + 33.79B + 10.68C - 2.83B^2 \quad (7)$$

$$\text{Young's modulus} = -171.76 + 5.65A + 75.55B - 6.16B^2 \quad (8)$$

Statistical analysis after model adjustment is presented in Tables VI and VII which illustrates that fitted models are significant for both strength ($P < 0.0001$) and Young's modulus ($P < 0.0001$). Tensile strength and Young's modulus of fibers obtained from experiments and predicted from the models are presented in Table V. The R^2 (0.8426), good agreement between R^2_{adj} (0.8006) and predicted R^2 (0.7340) and lack of fit ($P = 0.6288$) for tensile strength imply the quality of the model. Also the R^2 (0.7250), R^2_{adj} (0.6734), and lack of fit ($P = 0.2244$) values for Young's modulus indicate that the quadratic model is acceptable for the given experimental extent. Among all three factors the polymer concentration appeared to have the most significant effect on the mechanical properties of fibers. The importance of the solution concentration in controlling the mechanical properties of fibers has also been emphasized in other studies.[9,28] Fibers spun from lower concentration exhibited reduced mechanical properties indicating that a population of 'effective' chain entanglements is necessary to allow extension of intervening chain segments without the occurrence of chain slippage and molecular relaxation effects.[9] The spinning speed had quadratic effect on tensile strength and Young's modulus of fibers at applied experimental extent [Figure 6a,b]. These results

Table VIII. Analysis of Variance for Adjusted Model of (r_{av})

Source	Sum of squares	*df*	Mean square	*F* value	*P* value Prob > *F*	
Model	2646.84	9	294.09	24.22	<0.0001	Significant
$R^2 = 0.9353$						
$R^2_{adj} = 0.9232$						
$R^2_{pred} = 0.9019$						
Adequate precision = 28.391						
A Concentration (wt %)	1970.37	1	1970.37	176.06	<0.0001	
C Draw ratio	518.54	1	518.54	46.33	<0.0001	
A^2	100.26	1	100.26	8.96	0.0086	
Residual	179.06	16	11.19			
Lack of fit	139.14	11	12.65	1.58	0.3196	Not significant
Pure error	39.92	5	7.98			
Cor total	2768.24	19				

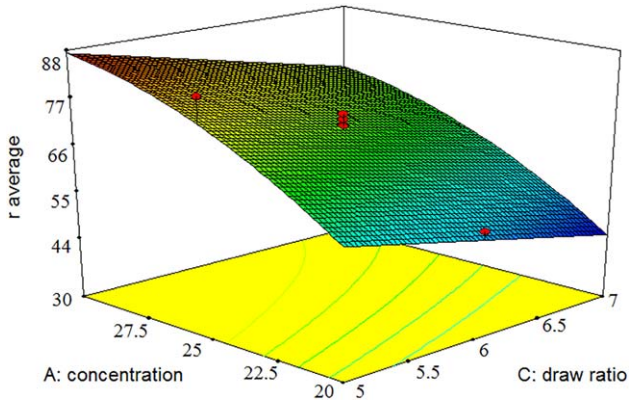

Figure 7. Response surface of the combined effects of solution concentration and draw ratio on r_{av}. [Color figure can be viewed in the online issue, which is available at wileyonlinelibrary.com.]

suggest that as the spinning speed is increased, the mechanical properties of fiber will increase until a critical level of shear is reached. It has been found that mechanical properties of fibers decreases if the extrusion is conducted above the point of fracture, which in some cases may occur at relatively low shear rates.[19] The quadratic effect also can be related to the effect of spinning speed on polymer chains orientation. The combination of solvent evaporation with shear and elongational stress as external fields can enhance the polymer chains orientation of fiber. Enhancement of the spinning speed leads to an increasing shear stress as well as shear rate at the spinneret which increase polymer chain orientation. By increasing of spinning speed from 3 to 5 cm/s, most population of polymer chains has orientated in the fiber axis therefore; increasing spinning speed up to 7 cm/s couldn't have more significant effect on polymer chain orientation as well as mechanical properties of fibers.

Increasing draw ratio increased fiber strength. Drawing of as-spun PCL fibers at room temperature essentially involves a process of breakdown and unfolding of crystalline units and extension of amorphous tie chain segments.[29] These changes in molecular organization result in the production of extended chain crystals and give rise to the oriented, fibrillar morphology of drawn PCL fibers.

Chain extension in the amorphous phase is facilitated by the low transition temperature T_g of PCL (−60°C), which ensures high chain mobility at room temperature.[9] The improvement in PCL fiber strength with increasing draw ratio can be related to the increase in molecular extension and alignment within the amorphous and crystalline phases of the fiber. However, it should be noted that in this work the draw ratio being defined as the ratio of take-up to extrusion velocity is actually a drawing down ratio. As it can be seen in Tables VI and VII, variation of drawing down ratio had less significant effect on tensile strength than concentration and spinning speed (lower F value).

Average Cross-Sectional Radius of Fibers

The cross sectional size (diameter) and cross sectional shape have direct effects on surface related properties of fibers as well as on many yarn and fabric properties. The diameter of fibers determines its total surface area and proportion of its surface, often termed surface-to-volume ratio (SVR). Properties that depend on the proportion of surface areas of fibrous products are expected to vary with fiber size.[30] As previously mentioned, the cross section of fibers was not perfectly circular and it was not possible to measure the diameter of a fiber in any meaningful way. Hence, an average cross sectional radius (r_{av}) was defined by following equation:

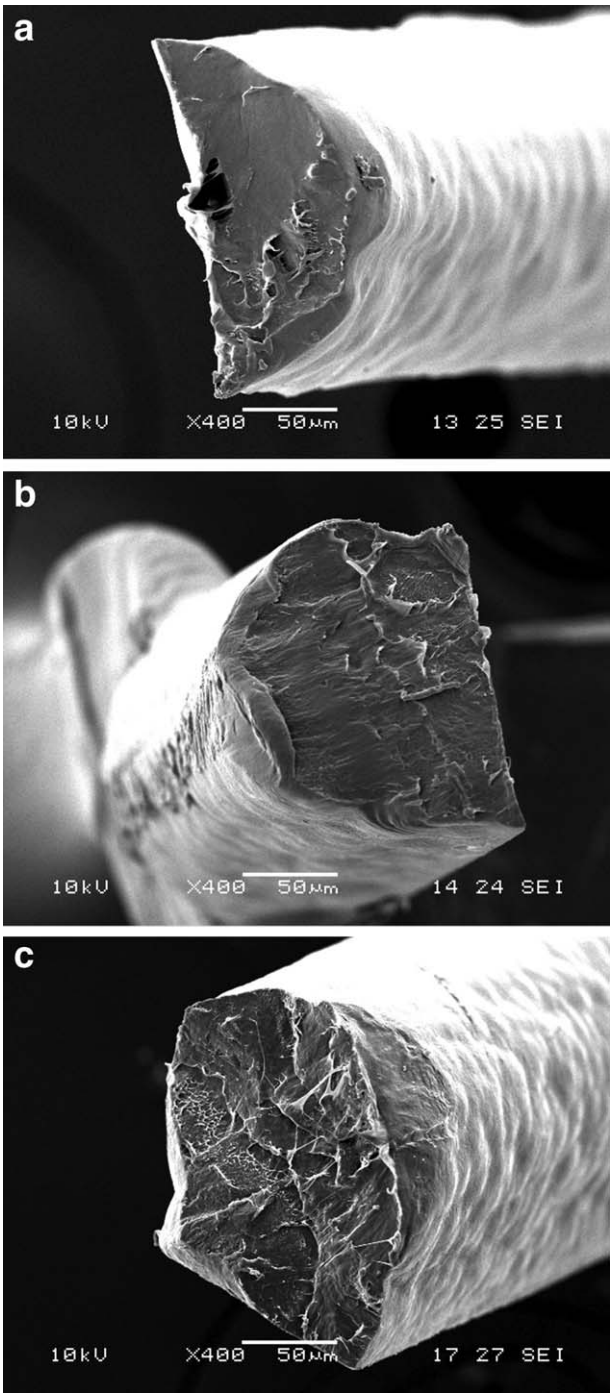

Figure 8. Cross-section of PCL fibers produce at spinning speed of 5 cm/s, draw ratio of 6 and concentration of (a) 20 wt %, b) 25 wt %, and (c) 30 wt %.

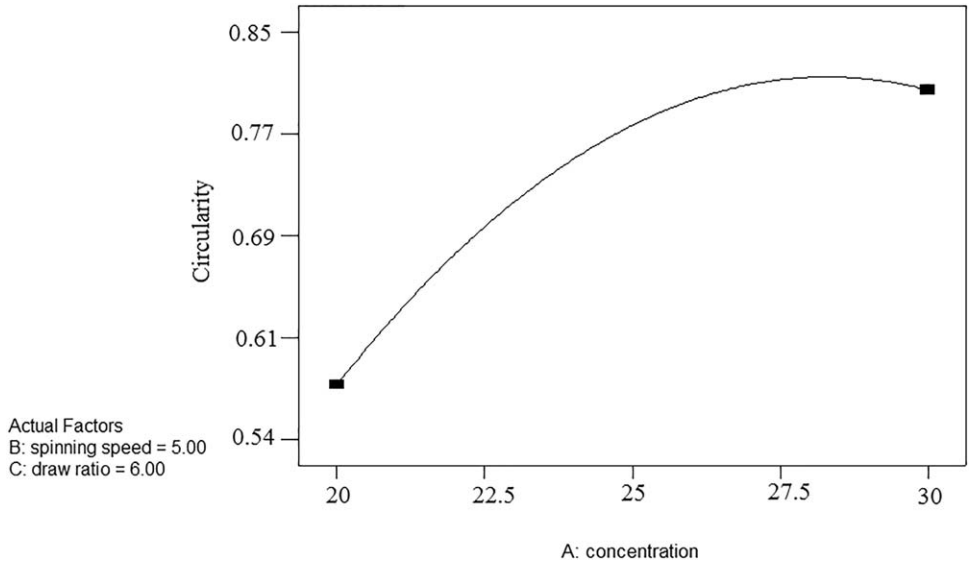

Figure 9. The effect of concentration on circularity of fibers.

$$r_{av} = 2/\mathrm{SVR} = 2 \times A/P \quad (9)$$

which is the radius of fiber with circular cross section and with the same SVR value of fiber with non circular cross section shape. The expression of SVR for a fiber of length L is:

$$\mathrm{SVR} = P \times L/A \times L = P/A \quad (10)$$

which P and A are the perimeter and the area of the cross section, respectively. For a fiber with a perfect circular cross section, SVR is:

$$\mathrm{SVR} = (2\pi r)\, L/(\pi R^2)\, L = 2/r \quad (11)$$

which r is radius of the fiber. Therefore, as it is obvious, SVR increases as cross-sectional size of the fiber decreases. SVR values were determined through analysis of the SEM images of fiber cross sections using Photoshop CS-5 software by measuring perimeter and area of cross sections. CCD was performed and a quadratic model was fitted to the results of r_{av} as response. The quadratic model was statistically reliable ($P < 0.0001$) and had no significant lack of fit ($P = 0.2211$). The relationship between the three factors and r_{av} was approximated by following quadratic equation:

$$r_{av} = -61.80 + 14.46A + 5.61B - 24.70C - 0.12AB - 0.20AC - 0.06BC - 0.19A^2 - 0.29B^2 + 1.90C^2 \quad (12)$$

The results of a statistical analysis show that just concentration and draw ratio had significant effect on r_{av}. Statistical analysis data after model reduction are presented in Tables VIII.

The F value of factor A (176.06) is bigger than the F value of factor C (46.33). Therefore, solution concentration (A) is the major factor affecting the r_{av} followed by draw ratio and spinning speed, in the order. By removing the insignificant parameters (B, AB, AC, BC, B^2, and C^2) eq. (12) is replaced by the following:

$$r_{av} = -68.37 + 11.76\,A - 7.20\,C - 0.17\,A^2 \quad (13)$$

The r_{av} of fibers obtained from experiments and predicted r_{av} from the model are presented in Table V. The quadratic effect of solution concentration can be clearly visualized in the

Table IX. Analysis of Variance for the Adjusted Model of Circularity

Source	Sum of squares	*df*	Mean square	*F* value	*P* value Prob > *F*	
Model	0.16	2	0.081	55.17	<0.0001	Significant
$R^2 = 0.8665$						
$R^2_{adj} = 0.8508$						
$R^2_{pred} = 0.8197$						
Adequate precision = 15.115						
A concentration (wt %)	0.13	1	0.13	85.68	<0.0001	
A^2	0.036	1	0.036	24.67	0.0001	
Residual	0.025	17	0.0014			
Lack of fit	0.014	12	0.0015	0.52	0.8367	Not significant
Pure error	0.011	5	0.0021			
Cor total	0.19	19				

response surface (Figure 7). Increasing concentration leads to increasing of r_{av} whereas by increasing draw ratio r_{av} decreased.

Circularity

There are various structural parameters (number of filament, cross-sectional shape, linear density, etc.) determined during the production of synthetic fiber and these parameters influence product features. Among these parameters, cross sectional shape of fibers has a significant importance. Desired features can be added to the products by varying the cross sectional shape and in this way new products with improved features or with high added value can be produced. As a consequence, studies on this subject have increased recently.[30] The shape factor is the ratio of the fiber perimeter of any cross-sectional shape to that of a circular shape at the same denier per filament (dpf) value.[31] Shape factors are often normalized, i.e., the value ranges from zero to one. A shape factor equal to one usually represents maximum symmetry, such as a circle. Deviation from the circular cross-sectional shape of a fiber gives a shape factor less than one. A very common shape factor is the circularity, a function of the perimeter P and the area A:

$$F_{circ} = 4\Pi A/P^2 \quad (14)$$

The circularity of a circle is 1.[32] In this study, the circularity of fibers was calculated using image analysis of cross section SEM images in Photoshop CS-5 software. To evaluate the influences of concentration, spinning speed and draw ratio on circularity of fibers, the design matrix of experimental conditions with the corresponding response values was fitted to a polynomial model and quadratic model was suggested. The mathematical equation proposed for this response (in terms of actual values) is:

$$\begin{aligned}\text{Circularity} = {} & -1.411+0.167A+0.023B-0.068C \\ & +1.25\times10^{-4}AB+2.25\times10^{-3}AC-6.25\times10^{-4}BC \\ & -3.18\times10^{-3}A^2-2.38\times10^{-3}B^2+4.54\times10^{-4}C^2\end{aligned} \quad (15)$$

Results show that just concentration had significant effect on circularity of fibers. Different solution concentrations, lead to different evaporation rate of the solvent in the air gap distance between the spinneret and take up roller. The higher the solvent inside the fiber, the higher deviation from circular cross-section shape (Figure 8).

The circularity of fibers obtained from experiments at different processing conditions and predicted circularity from the model are presented in Table V. The values determined were in agreement with the predicted values, which suggest that the model is accurate. Figure 9 shows the effect of concentration on circularity of fibers. As it can be seen, the circularity of fiber was more sensitive to changes at lower solution concentration. Analyzing the ANOVA results after model reduction is given in Table IX and the final model after removing insignificant parameters (B, C, AB, AC, BC, B^2, and C^2) was refined as follows:

$$\text{Circularity} = -1.90+0.192A-3.4\times10^{-3}A^2 \quad (16)$$

These statistical results reveal that developed CCD for the prediction of circularity is statistically validated for the approximation of response over the range of experimentation considered (valid region).

CONCLUSIONS

The main objective of our research is to examine the influence of concentration, spinning speed, and draw ratio on PCL fibers properties. Response surface methodology based on a three-level, three-factor central composite design (CCD) was implemented to determine the significant factors that affect the response and to develop mathematical equation for the optimization. The ANOVA results indicated that the linear density of fibers was most suitably described with a quadratic model and it depended on all three processing parameter. CCD was performed on experimental data of strength and Young's modulus of fibers and quadratic models were fitted to the results. Statistical analysis revealed that polymer concentration had the most significant effect on tensile strength and on Young's modulus of the fibers. A quadratic model was fitted for r_{av} and circularity. Spinning speed had no significant effect on r_{av}. Only polymer concentration had a dramatic effect on circularity of fiber and it was more sensitive to changes at lower solution concentration. Response surface methodology is a powerful statistical technique for testing multiple variables. In particular, fewer experimental trials are needed as compared to the "one-factor-at-a-time" method. Moreover, the use of this model allows a straightforward and systematic representation of the process parameters influencing fiber formation, and can be used to predict the results of fiber spinning carried out using different combinations of process parameters.

ACKNOWLEDGMENTS

Dr. Randa Ishak is gratefully acknowledged for performing SEM analysis. This research was funded in part by Italian Ministry of Education, University and Research, grant PRIN 2010 SNALEM.

REFERENCES

1. Azimi, B.; Nourpanah, P.; Rabiee, M.; Arbab, S. *J. Eng. Fiber. Fabr.* **2014**, *9*, 74.
2. Williamson, M. R.; Chang, H. I.; Coombes, A. G. A. *Biomaterials* **2004**, *25*, 5053.
3. Tomihata, K.; Suzuki, M.; Oka, T; Ikada, Y. *Polym. Degrad. Stabil.* **1998**, *59*, 13.
4. Yoshimoto, H.; Shin, Y. M.; Terai, H.; Vacanti, J. P. *Biomaterials* **2003**, *24*, 2077.
5. Charuchinda, A.; Molloy, R.; Siripitayananon, J.; Molloy, N.; Sriyai, M. *Polym. Int.* **2003**, *52*, 1175.
6. Puppi, D.; Detta, N.; Piras, A. M.; Chiellini, F.; Clarke, D. A.; Reilly, G. C.; Chiellini, E. *Macromol. Biosci.* **2010**, 887.
7. Williamson, M. R.; Adams, E. F.; Coombes, A. G. A. *Eur. Cells Mater.* **2002**, *4*, 62.
8. Arbab, S.; Noorpanah, P.; Mohammadi, N.; Soleimani, M. *J. Appl. Polym. Sci.* **2008**, *109*, 3461.
9. Williamson, M. R.; Coombes, A. G. A. *Biomaterials* **2004**, *25*, 459.
10. Chang, H. I.; Lau, Y. C.; Yan, C.; Coombes, A. G. A. *J. Biomed. Mater. Res. A* **2008**, *84*, 230.

11. Puppi, D.; Mota, C.; Gazzarri, M.; Dinucci, D.; Gloria, A.; Myrzabekova, M.; Ambrosio, L.; Chiellini, F. *Biomed. Microdev.* **2012**, *14*, 1115.
12. Arbab, S.; Mohammadi, N.; Noorpanah, P. *Polymers* **2008**, *8*, 935.
13. Arbab, S.; Noorpanah, P.; Mohammadi, N.; Zeinolebadi, A. *Polym. Bull.* **2011**, *66*, 1267.
14. Rajabian, M.; Koll, J.; Buhr, K.; Handge, U. A.; Abetz, V. *Polymer* **2013**, *54*, 1803.
15. Puppi, D.; Piras, A. M.; Chiellini, F.; Chiellini, E.; Martins, A.; Leonor, I. B.; Neves, N.; Reis, R. *J. Tissue Eng. Regen. Med.* **2011**, *5*, 253.
16. Qin, J.-J.; Chung, T.-S. *J. Membr. Sci.* **2004**, *229*, 1.
17. Ismail, A. F.; Yean, L. P. *J. Appl. Polym. Sci.* **2003**, *88*, 442.
18. Montgomery, D. C. Design and Analysis of Experiments, 8th ed; Wiley: New York, **2012**.
19. Walczak, Z. K. Processes of Fiber Formation; Elsevier: Oxford, **2002**.
20. Bezerra, M. A.; Santelli, R. E.; Oliveira, E. P.; Villar, L. S.; Escaleira, L. E. *Talanta* **2008**, *76*, 965.
21. Steenackers, G.; Presezniak, F.; Guillaume, P. *Comput. Ind. Eng.* **2009**, *57*, 847.
22. Solouk, A.; Solati-Hashjin, M.; Najarian, S.; Mirzadeh, H.; Seifalian, A. M. *Iran. Polym. J.* **2011**, *20*, 91.
23. Saville, B. P. Physical Testing of Textiles; Woodhead Publishing: Manchester, **1999**.
24. Sommerville, P. J. Fundamental Principles of fibre fineness Measurements. Part 2. Understanding Fiber Diameter Measurment, Australian Wool Testing Authority Ltd: Melbourne, Australia, **2002**, p 1–5.
25. Roso, M.; Lorenzetti, A.; Besco, S.; Monti, M.; Berti, G.; Modesti, M. *Comput. Chem. Eng.* **2011**, *35*, 2248.
26. Park, S.; Kim, B.; Xu, J.; Hofmann, T.; Ocko, B.; Russell, T. P. *Macromolecules* **2009**, *42*, 1278.
27. Ismail, A. F.; Yean, L. P. *J. Appl. Polym. Sci.* **2003**, *88*, 442.
28. Gogolewski, S.; Pennings, A. J. *J. Appl. Polym. Sci.* **1983**, *28*, 1045.
29. Mark, H. F.; Sheldon, M.; Atlas, E.; Eds. Man Made Fibers: Science and Technology; Wiley: New York, **1968**.
30. Pastore, C.; Kiekens, P.; Eds. Surface Characteristics of Fibers and Textiles, Surfactant Science Series, Vol. *94*; Marcel Dekker: New York, **2001**.
31. Babaarslan, O.; Hacioğullari, S. Ö. *Fiber. Polym.* **2013**, *14*, 146.
32. Montero, R. S. *Int. Math. Forum* **2009**, *4*, 1305.